

Band gap engineering of MoS₂ upon compression

Miquel López-Suárez,¹ Igor Neri,^{1,2} and Riccardo Rurali³

¹*NiPS Laboratory, Dipartimento di Fisica e Geologia,
Università degli Studi di Perugia, 06123 Perugia, Italy**

²*INFN Sezione di Perugia, via Pascoli, 06123 Perugia, Italy*

³*Institut de Ciència de Materials de Barcelona (ICMAB-CSIC)
Campus de Bellaterra, 08193 Bellaterra, Barcelona, Spain*

(Dated: February 16, 2022)

Abstract

Molybdenum disulfide (MoS₂) is a promising candidate for 2D nanoelectronic devices, that shows a direct band-gap for monolayer structure. In this work we study the electronic structure of MoS₂ upon both compressive and tensile strains with first-principles density-functional calculations for different number of layers. The results show that the band-gap can be engineered for experimentally attainable strains (i.e. ± 0.15). However compressive strain can result in buckling that can prevent the use of large compressive strain. We then studied the stability of the compression, calculating the critical strain that results in the on-set of buckling for free-standing nanoribbons of different lengths. The results demonstrate that short structures, or few-layer MoS₂, show semi-conductor to metal transition upon compressive strain without buckling.

* miquel.lopez@nipslab.org

I. INTRODUCTION

Molybdenene disulfide, MoS₂, is a Transition Metal Dichalcogenide, TMD, with a hexagonal structure like graphene [1]. As in the case of graphene, MoS₂ can be exfoliated down to a single sheet [2, 3] composed by one layer of Mo atoms stacked between two sulfide layers (see Fig.1(a)). Single layer MoS₂ is a direct gap semiconductor [4] with $E_g = 1.9$ eV and high stiffness which makes it a very promising material for new nano electromechanical devices [5]. Layered materials of this class are especially amenable to band-gap engineering upon strain, and monolayer and bilayer MoS₂, in particular, have been shown to ultimately undergo a semiconductor-metal transition by means of mechanical strain [6]. This transition occurs for tensile strains of around $\varepsilon = 0.1$, where $\varepsilon = \delta l/l$, with l the original length of the structure. The effect of compressive strain, however, has been thus far neglected. The reason are twofold: (i) experiments are naturally performed applying a tensile strain; (ii) compression is, at least in principle, a source of structural instability in a two dimensional material, as it can result in buckling or other types of out-of-plane deformations [7].

In this work we present first-principles electronic structure calculations of monolayer, bilayer, few-layer and bulk MoS₂ under axial and biaxial compressive strains of up to $\varepsilon = 0.15$. We explicitly address the stability of monolayer MoS₂ upon compression, calculating the threshold strain beyond which the accumulated elastic energy is relaxed through buckling of the system. Additionally, we also extend the known results of MoS₂ under tensile strain [6, 8] considering mono-, few-layer and bulk MoS₂, showing that these systems too can experience semiconductor-metal transition considering strains from $\varepsilon = 0.08$ to $\varepsilon = 0.12$, that can be achieved in the experiments (i.e. $\varepsilon = 0.23$) [9].

II. METHODS

First principles calculations are carried out within Density Functional Theory (DFT), as implemented in the SIESTA package [10]. We use the Perdew-Burke-Eznerhof parameterization of the Generalized Gradient Approximation (GGA) [11] and an optimized double- ζ polarized basis set to expand the one-electron wave-function. Core electrons are accounted for by means of norm-conserving pseudopotentials. A converged grid of k -points to sample the Brillouin zone (the number of points and the direction of the reciprocal space samples depend on the dimensionality and cell size of the different systems studied, i.e. layered 2D

materials, bulk or nanotube) is used. All structures are relaxed until all forces are lower than 0.04 eV/Å. The unit-cells of mono-layer and bulk MoS₂ are shown in Fig. 1(a). The values for the lattice constant for the different structures considered in this work are listed in Table I, which are in good agreement with the literature [12]. Strain is introduced to the system by deforming the unit-cell along the x and y axis for biaxial strain while deformation only along the x -axis is considered for uniaxial strain. In the case of uniaxial strain we study both the case in which the unstrained lattice vector is and is not optimized. The former gives access to the Poisson's ratio, besides the Young's modulus; the latter more closely models the situation in which a MoS₂ layer is strongly adhered to a mismatched substrate that compresses it only along one direction, but not along the other. The band structures of all unstrained structures present an indirect band gap except that for mono-layer MoS₂ which exhibits a direct band gap placed at the K point, also in good agreement with previous studies [4]. The energy band gap, E_g , as a function of the number of layers is shown in Fig. 1(b).

III. RESULTS

The dependence of E_g for monolayer MoS₂ with compressive and tensile strain is shown in Fig. 2. Both tensile and compressive strain produce a reduction of the band gap, regardless whether it is uniaxial or biaxial. In particular, biaxial compressive strain is the more effective way to tune the band gap and to ultimately drive a transition from semiconducting to metallic character, occurring at $\varepsilon = -0.14$, while the less effective method is compressive uniaxial strain, where E_g shrinks of at most 1 eV for the largest values of the strain considered. Free standing monolayers –where upon uniaxial compression the sheet is free to transversely expand (see Fig. 2 (b))– are slightly less sensitive to the applied strain, though the differences become negligible at high compressions.

A close inspection reveals a change of slope in the decrease of the band gap as a function of biaxial strain around $\varepsilon = -0.08$. In order to understand this behavior we have tracked the dependence on the compressive strain of a few eigenvalues at high symmetry points (see the band-structure diagram of Fig. 3(a) for labeling). It turns out that the valence band maximum at the M point increases much more quickly than the one at K and for compressive strains larger than ~ -0.08 it becomes the absolute maximum of the valence band. Therefore, the shrinking of band gap is determined by the pressure coefficient of the

valence band at M , while the larger pressure coefficient of the K point takes over at larger compression. A tiny compressive strain, on the other hand, is sufficient to have the minimum of the conduction band at a point on the $\Gamma - K$ path (ΓK_c), approximately equidistant from the two ends. This can be seen in the inset of Fig. 3(b) where we have expanded the small strain region ($|\varepsilon|$ smaller than 0.01). Therefore, the band gap remains direct at the K point only for $-0.005 < \varepsilon < 0$; when $-0.08 < \varepsilon < -0.005$ the gap is indirect because the minimum of the conduction is along the $\Gamma - K$ path; finally, for $\varepsilon < -0.08$ is indirect between M and $\Gamma - K$. The same behavior is present also for the uniaxial strain, relaxed and not, even though the minimum indirect gap is for different paths respect to the biaxial case.

These results indicate that the band gap of monolayer MoS₂ can be engineered through compressive strain, similarly to what has been already shown with tensile strain. The response to strain is of the same order in both cases. However, one of the reasons that make compressive strain a less appealing way to engineer the band gap is that, at variance with tensile strain, at a high enough compression the flat geometry becomes unstable and buckling of the two-dimensional system is favored. While these buckled geometries can be useful for non-linear energy harvesting of vibrational energy, as reported previously by some of us [13–15], they are far to be ideal from the device design viewpoint of, say, a field-effect transistor. Atom-thick graphene buckles even for very small strain values [13], but previous reports hinted that for MoS₂ the flat geometry remains stable in a non-negligible range of compression [16].

In order to find the maximum compression that a ribbon of length l can support before buckling, we have compared the total energy under bending and under in-plane compression. The energy per unit formula (E_U) of MoS₂ under bending has been calculated considering nanotubes of different radius R . The energy as function of the curvature radius varies as $1/R^2$, as shown in Fig. 4(a). When a ribbon buckles the curvature along its length is not constant and therefore the energy must be computed accordingly to the resulting curvature. In order to do so, we assume that the out-of-plane atomic displacements follow $u(x) = A \sin(2\pi/lx)$ and that the total length of the ribbon is constant and equal to its initial value, l . The energy per unit formula of a MoS₂ as function of in-plane compression is shown in Fig. 4(b) (red circles), and can be approximated to $E_U = k1/2Y\varepsilon^2$, where Y is the Young's modulus and ε is the in-plane strain.

The critical strain, ε_c , is the strain at which buckling becomes more favorable than in-

plane compression. This is shown in Fig. 4(b) as crossing points between the red line and the different lines corresponding to the bending energy for different ribbon lengths. The model agrees well with the prediction of Euler elasticity theory, black continuous line in Fig. 4(b), to be compared with the black squares, i.e. the critical strains obtained from the data.

It seems clear that, for monolayer MoS₂, compressions larger than -0.05 can be achieved without buckling only for nanoribbons shorter than 3 nm. Ribbons with more attainable dimensions, i.e. $l > 100$ nm, buckle for $\varepsilon < -0.001$ which effectively prevent the modulation of the band-gap by compressive strain. Nonetheless, the bending energy increases for thicker structures, i.e. bi-layer, tri-layer, approaching infinite for bulk materials. The critical strain ε_c also increases, widening the range of compressive strains can be attained without inducing buckling, even in systems of longer lengths. For this reason, we have also calculated the response to strain of few-layer and bulk MoS₂, finding a qualitative similar behavior (see Fig. 5). Our results show not only a decrease of the energy band gap for unstrained few-layer MoS₂ (reaching $E_g = 1$ eV for bulk), but also the possibility of achieving a semiconductor-to-metal transition for high applied compressive strains in all cases. Noteworthy, the transition occurs even for slightly lower strain values, both compressive and tensile, for increasing number of layers. As a final remark one should note that, while predictions of the pressure coefficients based on DFT calculations are very reliable, the band-gaps are notoriously underestimated. This means that the slopes of the curves in Fig. 2 and 5 are accurate, but closing the band-gap likely requires larger strains.

IV. CONCLUSIONS

In conclusion, we have shown that both tensile and compressive strain result in band gap engineering of monolayer, few-layer and bulk MoS₂. A transition from semiconductor to metal can be achieved for compressions of the order of $\varepsilon = 0.13$ for monolayer MoS₂ under biaxial strain, while for bulk MoS₂ this value is reduced to 0.10. We have also computed the maximum compression that a MoS₂ monolayer can stand without favoring the onset of buckling instabilities, thus assessing within which range compressive strain can be used to tailor the electronic properties of a flat MoS₂ sheet. From the latter calculations we show that the maximum dimensions for single layer MoS₂ able to show a metal transition before bucking are impracticable (i.e. maximum 3 nm). However the bucking can be avoided considering few-layer suspended structures, that also show semiconductor to metal transition, or the

confinement of the MoS₂ to a substrate, which can also delay the emergence of buckling.

ACKNOWLEDGMENTS

MLS and IN gratefully acknowledge financial support from the European Commission (FPVII, Grant agreement no: 318287, LANDAUER and Grant agreement no: 611004, ICT-Energy). RR acknowledges the Severo Ochoa Centres of Excellence Program under Grant SEV-2015-0496, funding under contracts Nos. FEDER-MAT2013-40581-P of the Ministerio de Economía y Competitividad (MINECO) and grant 2014 SGR 301 of the Generalitat de Catalunya.

-
- [1] Q. H. Wang, K. Kalantar-Zadeh, A. Kis, J. N. Coleman, and M. S. Strano, *Nat. Nanotech.* **7**, 699 (2012).
- [2] H. Li, J. Wu, Z. Yin, and H. Zhang, *Acc. Chem. Res.* **47**, 1067 (2014).
- [3] N. Liu, P. Kim, J. H. Kim, J. H. Ye, S. Kim, and C. J. Lee, *ACS Nano* **8**, 6902 (2014).
- [4] K. F. Mak, C. Lee, J. Hone, J. Shan, and T. F. Heinz, *Phys. Rev. Lett.* **105**, 136805 (2010).
- [5] S. Bertolazzi, J. Brivio, and A. Kis, *ACS Nano* **5**, 9703 (2011).
- [6] P. Johari and V. B. Shenoy, *ACS Nano* **6**, 5449 (2012).
- [7] K. Zhang and M. Arroyo, *J. Mech. Phys. Solids* **72**, 61 (2014).
- [8] W. S. Yun, S. W. Han, S. C. Hong, I. G. Kim, and J. D. Lee, *Phys. Rev. B* **85**, 033305 (2012).
- [9] R. C. Cooper, C. Lee, C. A. Marianetti, X. Wei, J. Hone, and J. W. Kysar, *Phys. Rev. B* **87**, 035423 (2013).
- [10] J. M. Soler, E. Artacho, J. D. Gale, A. García, J. Junquera, P. Ordejón, and D. Sánchez-Portal, *J. Phys.: Condens. Matter* **14**, 2745 (2002).
- [11] J. P. Perdew, K. Burke, and M. Ernzerhof, *Phys. Rev. Lett.* **77**, 3865 (1996).
- [12] C. Ataca, M. Topsakal, E. Akturk, and S. Ciraci, *J. Phys. Chem. C* **115**, 16354 (2011).
- [13] M. López-Suárez, R. Rurali, L. Gammaitoni, and G. Abadal, *Phys. Rev. B* **84**, 161401 (2011).
- [14] M. López-Suárez, R. Rurali, and G. Abadal, *Microelectronic Engineering* **111**, 122 (2013).
- [15] M. López-Suárez, M. Pruneda, G. Abadal, and R. Rurali, *Nanotechnology* **25**, 175401 (2014).
- [16] M. López-Suárez, *Energy harvesting from the microscale to the nanoscale*. PhD Thesis, 2015. <http://hdl.handle.net/10803/283731>.

TABLE I. Values for the lattice constant for different number of layers

	1L	2L	3L	4L	Bulk
a (\AA)	3.18	3.20	3.20	3.20	3.20

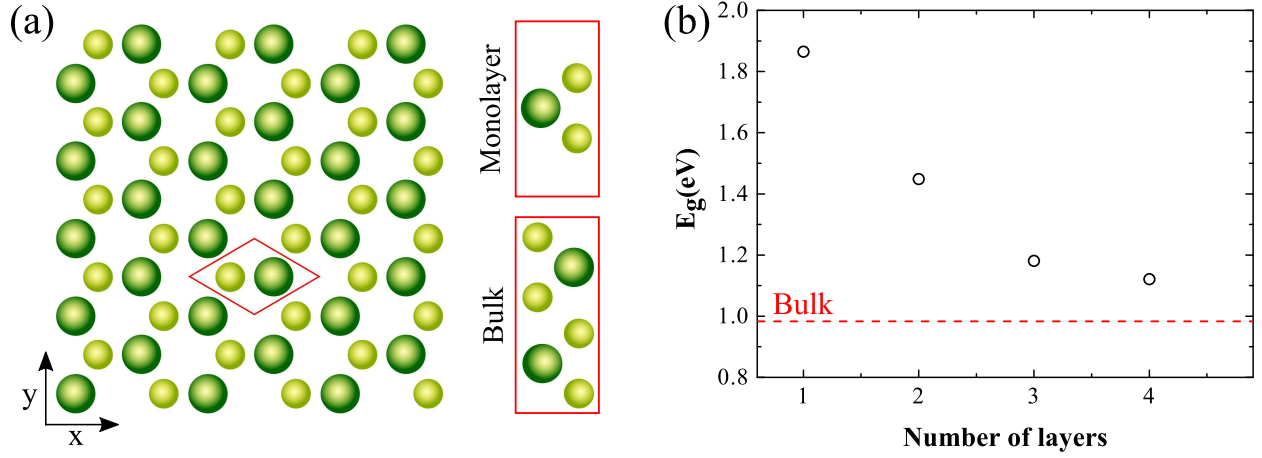


FIG. 1. (a) MoS₂ structure: red boxes highlight the primitive cells for top view (rhombus), and lateral views for mono layer and bulk (rectangles). (b) Energy gap for various number of layers (dots) and bulk (dashed line) MoS₂.

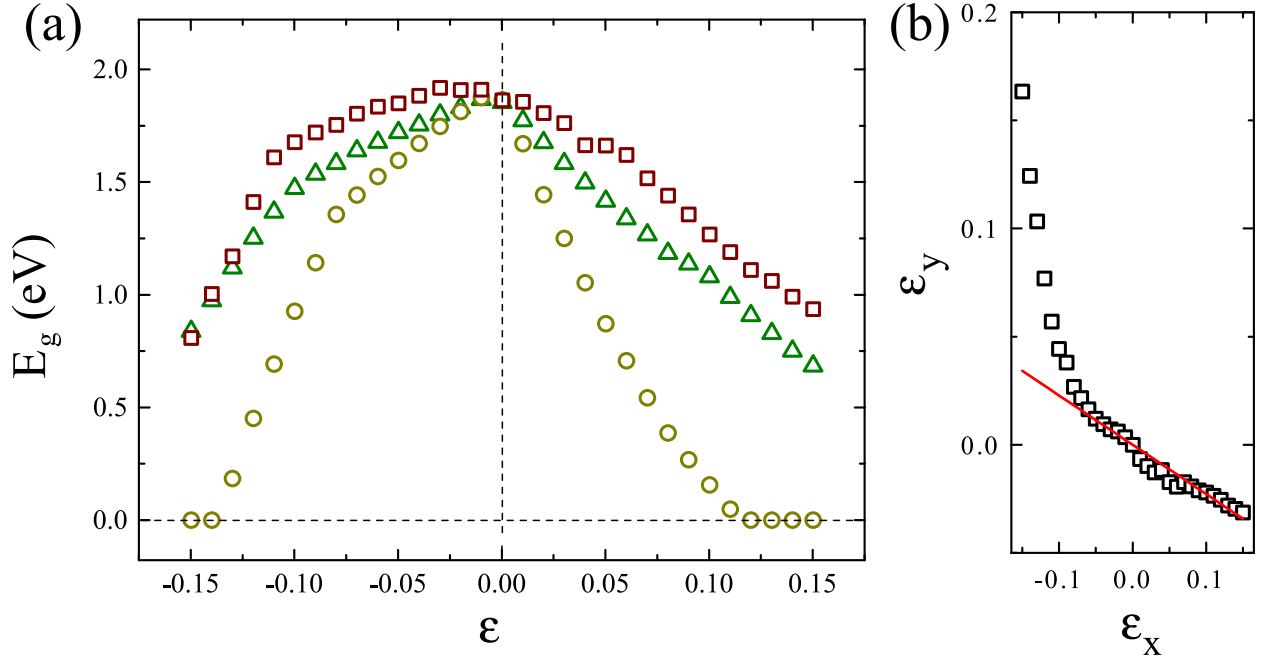


FIG. 2. (a) Dependence of the band gap of a monolayer of MoS₂ as a function of the applied biaxial strain (circles) and uniaxial strain when the material is (squares) and is not (triangles) free to expand/contract in the perpendicular direction. (b) Induced strain along y as a function of the applied strain along x in the case of uniaxial strain of a free standing MoS₂ monolayer (squares in panel (a)). We found a negative ratio of transverse to axial strain resulting in a Poisson's ratio, ν , of 0.23.

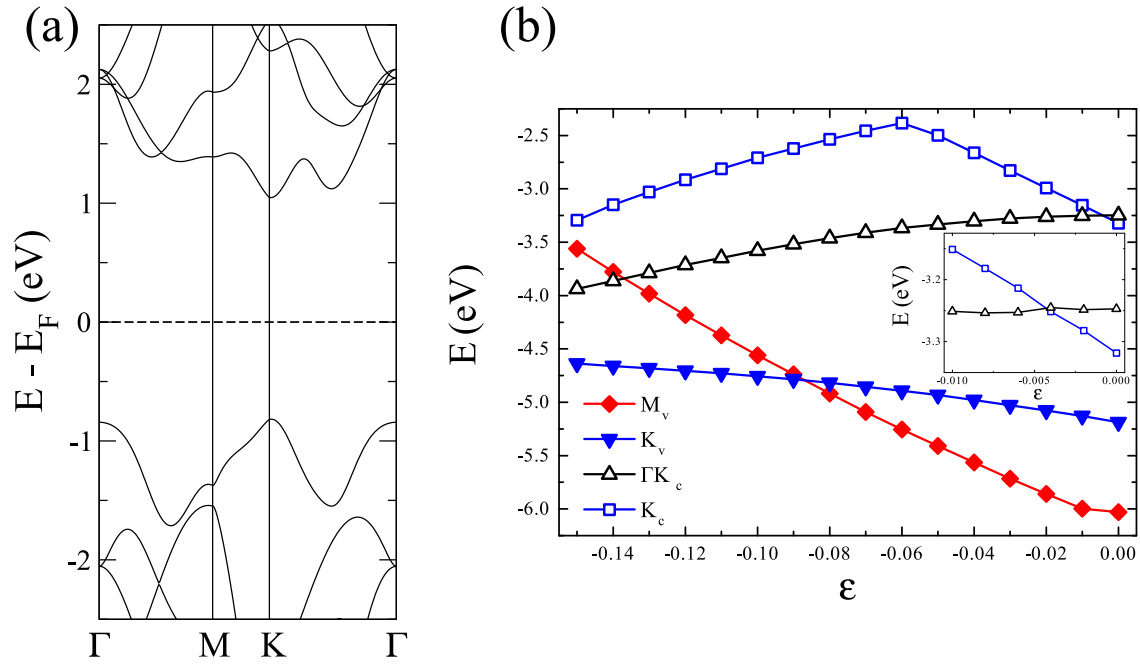


FIG. 3. (a) Band-structure diagram of an unstrained MoS₂ monolayer. (b) Dependence of the band-edge eigenvalues as a function of biaxial strain; inset: zoom of the low strain region where the band gap becomes indirect.

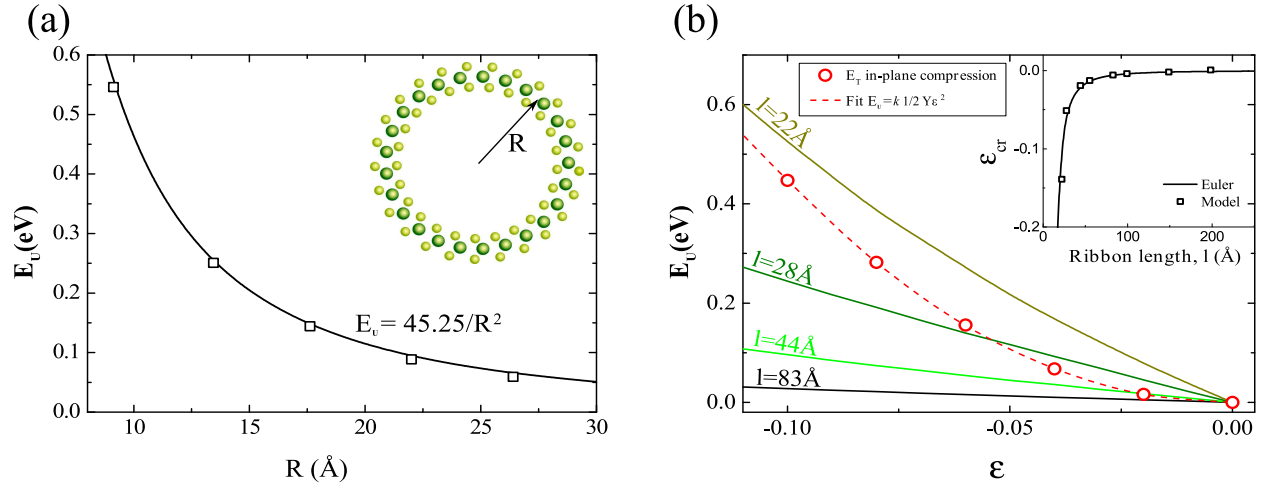


FIG. 4. (a) Curvature energy: energy per unit formula (E_U) of a MoS₂ nanotube as a function of the radius. (b) Comparisons between in-plane compression (red circles, dashed line is the fit) and buckling for different lengths, l , (continuous lines); inset: critical strains at which buckling is favored.

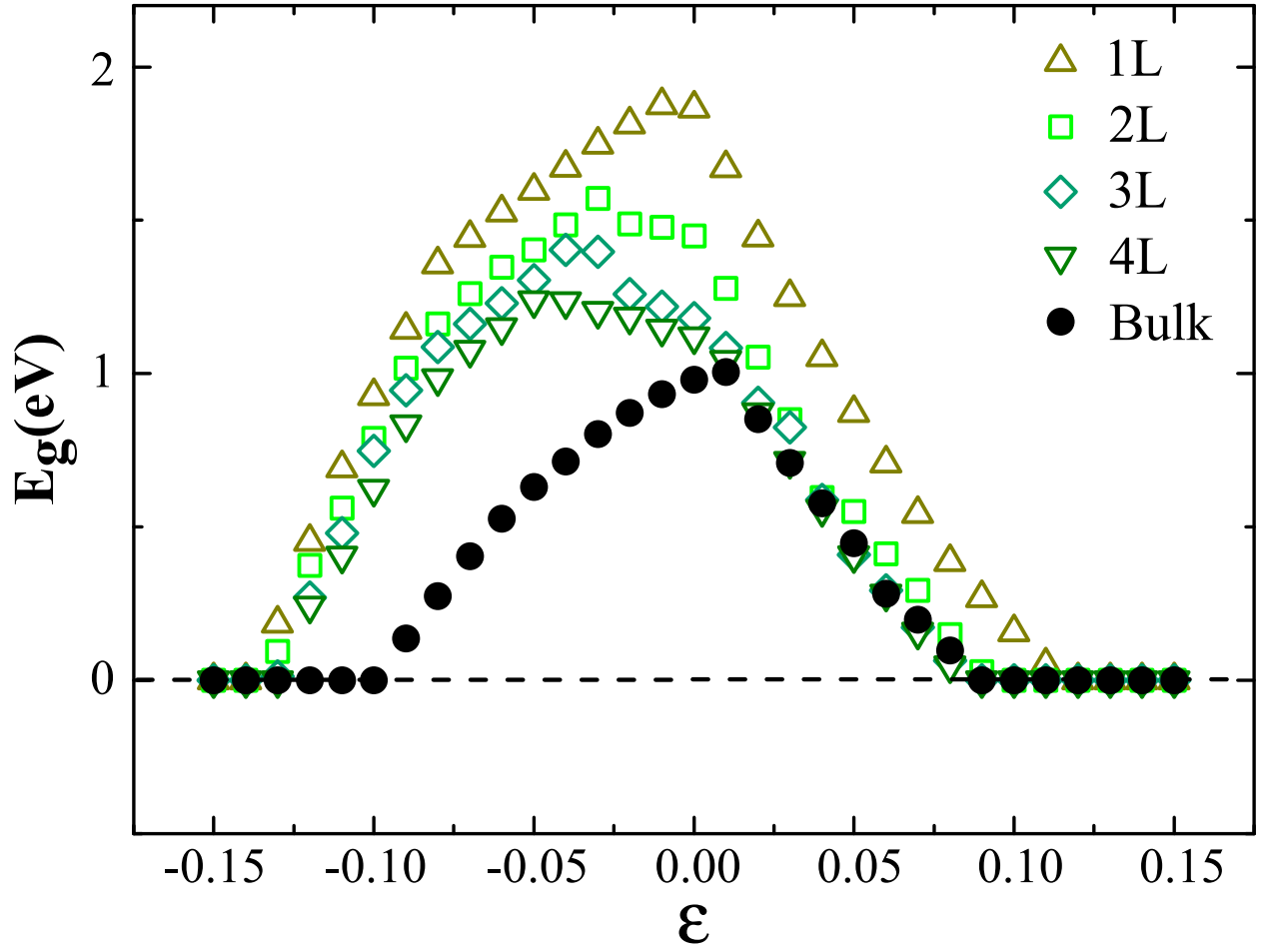


FIG. 5. Energy gap for mono, few-layer, and bulk MoS₂ as function of biaxial strain. For bulk material metal transition occurs at lower compressive strain compared to mono and few-layer. For stretching strains the transition appears at $\epsilon \sim 0.08$ for bulk and few-layer MoS₂.